

DESIGN AND EXPERIMENT OF GRAIN HARVESTER YIELD MONITORING SYSTEM BASED ON MULTI-SENSOR FUSION

基于多传感器融合的谷物收割机产量监测系统的设计与实验

Peng LIU ¹⁾, Shijun SONG ¹⁾, Wei LIU ¹⁾, Yuqian ZHAO ¹⁾, Weichen YAN ¹⁾, Guohai ZHANG ^{1,2*)}

¹⁾Shandong University of Technology, Collage of Agricultural Engineering and Food Science, Zibo, China

²⁾Shandong University of Technology, Institute of Modern Agricultural Equipment, Zibo, China

Tel: +86119862513808; E-mail: guohaizhang@sdut.edu.cn

Corresponding author: Guohai Zhang

DOI: <https://doi.org/10.35633/inmateh-75-65>

Keywords: Harvester yield monitoring system; Optical yield measurement; Weighing yield measurement; Self-feedback system

ABSTRACT

Precision agriculture requires accurate and efficient crop yield distribution information. However, both traditional field-based yield measurement methods and existing combine harvester yield monitoring systems face significant limitations. Traditional methods, such as direct weighing or sampling, are time-consuming and inefficient, and they only provide average yield values - insufficient for large-scale farming needs. Meanwhile, current monitoring systems often suffer from high measurement errors, low spatial resolution, and limited generalizability. For this reason, this study designs a new type of grain yield monitoring system, which corrects the photoelectric sensor data through the load cell data, realizes the calibration of the photoelectric sensor, avoids the influence of external factors, and improves the accuracy of measurement. Firstly, tests were carried out at three rotational speeds of 10 Hz, 20 Hz and 25 Hz of the motor inverter setting, respectively, to determine the positive proportionality coefficient between the photoelectric signal and the grain mass, and the overall error of the system was measured to be less than 6.44%. For the load cell, a model of the relationship between tilt angle and weighing accuracy was established and a compensation algorithm was proposed, the weighing error data in different directions and at different tilt angles were measured and analyzed, and a mathematical model between the corrected angle and the weighing error was established. Through the tilting experiment, the feasibility of the modified angle compensation model is verified, and the overall error after compensation is less than 0.25%, and the systematic error of measurement and production after the intervention of the feedback system is less than 0.74%. The experimental results demonstrate that the system significantly enhances the accuracy and stability of yield measurement. It holds substantial potential for widespread application, provides strong support for the advancement of precision agriculture, and is expected to drive agricultural production toward greater efficiency and sustainability.

摘要

精准农业需要准确且高效的作物产量分布信息，但传统的田间作物产量获取方法以及现有的联合收割机产量监测系统存在诸多问题。传统方法，如直接称重或抽样，不仅耗时且效率低下，而且只能获取平均产量，难以满足大面积种植的需求，而现有的系统测量误差大、空间分辨率低且通用性差。为此，本研究设计了一种新型的谷物产量监测系统，该系统通过称重传感器数据对光电传感器数据进行校正，实现了对光电传感器的校准，避免了外部因素的影响，提高了测量精度。首先，分别在电机变频器设定的10赫兹、20赫兹和25赫兹这三种转速下进行测试，以确定光电信号与谷物质量之间的正比例系数，经测量该系统的整体误差小于6.44%。对于称重传感器，建立了倾斜角度与称重精度之间关系的模型，并提出了一种补偿算法，测量并分析了不同方向和不同倾斜角度下的称重误差数据，建立了校正角度与称重误差之间的数学模型。通过倾斜实验，验证了修正后的角度补偿模型的可行性，补偿后的整体误差小于0.25%，反馈系统介入后测量和生产的系统误差小于0.74%。实验结果表明，该系统有效地提高了产量测量的准确性和稳定性，具有广泛的应用价值，为精准农业的发展提供了有力支持，有望推动农业生产朝着更高效、更可持续的方向发展。

INTRODUCTION

Precision agriculture, also known as smart agriculture, is an agricultural management method that integrates modern information technologies such as geographic information system (GIS), global positioning system (GPS), remote sensing technology, and Internet of Things (IoT) (Luo *et al.*, 2001; Maldaner *et al.*, 2021; Maldaner *et al.*, 2022; Price *et al.*, 2017; Sirikun *et al.*, 2021; Wang *et al.*, 2021; Yin *et al.*, 2024). It realizes precise control of the agricultural production process, including precise fertilization, irrigation, and harvesting, through real-time monitoring and data analysis of the farmland environment, crop growth, and soil conditions. In the process of crop cultivation and production management, obtaining the information of crop yield distribution in the farmland in an online, real-time, and effective method is the main starting point for the implementation of precision agriculture (Li *et al.*, 2004; Lou *et al.*, 2006). The traditional method of obtaining field crop yields is through direct weighing or sampling, which is not only time-consuming and inefficient, but also can only obtain the average yield of crops, so it is not suitable for obtaining the yields of field crops planted over large areas. The use of remote sensing technology to collect crop images or establish crop growth condition models are extracted crop characteristic values to establish the relationship with crop yield, but the collected data are affected by environmental factors (Choi *et al.*, 2018; Martello *et al.*, 2022; Taylor *et al.*, 2016). In field harvesting operations, real-time information on crop yield distribution in large fields can be accurately obtained through instantaneous yield monitoring of the combine harvester operation process. Through the drawn spatial distribution map of farmland yield, subsequent field management, rational use of agricultural resources, regulation of input-output ratio, improve yield, reduce pollution, is the basic guarantee of sustainable development of agricultural production (Wang *et al.*, 2021).

Currently, grain yield monitoring techniques mainly include impact measurement, volumetric measurement, dynamic weighing measurement, and radiation measurement, etc. Zandonadi *et al.*, (2009), verified the correlation between the tension on the tension side of the bin chain, shaft torque, and yield by setting a torque sensor in the bin of a harvester. The maximum error of the yield monitoring system designed in this way was 4.9%. Geng *et al.*, (2021), developed an on-line monitoring system for on-board grain yield based on the principle of grain flow pressure, guided by the mathematical model of grain yield and grain flow pressure. They built a grain yield monitoring test bed and investigated the effects of the number of sensors, the sensor installation position, and the horizontal inclination angle of the monitoring device on the yield measurement error of the grain yield monitoring system. The results showed that the indoor test error of the grain yield monitoring system was 3.27% and the field yield measurement error was 5.28%. Fang *et al.*, (2024), designed a convex surface grain mass flow sensor to compare the errors of different grain types and flow rates on the experimental measurements, and the measurement error was less than 5% after calibrating the zero point and coefficient of the sensor. Cheng *et al.*, (2023), constructed a corn seed yield model based on low-potential signals by adding three pairs of photoelectric sensors to a scraper—type elevator of a corn kernel harvester and achieved real-time monitoring of yield. The average error of the measured yield was 3.72%. Navid *et al.*, (2015), utilized a laser line scanner to measure material flow. In the system, the laser line scanner measures the distance between the sensor and the object according to the time-of-flight principle. Grain flows from a stationary bin, and a sliding door at the bottom of the bin is used to regulate the mass flow rate of grain. The results showed that the grain flow rate and the laser scanning signal are linearly related. This method is one of the yield measurement methods. Overall, the study shows that there is no significant difference in the measurement errors of different yield measurement methods, and the main sources of error include: non—calibration error, sensor response error, grain moisture content measurement error, and error due to uneven distribution of grain flow.

Existing combine harvester yield monitoring systems usually employ impact grain flow sensors, photoelectric volumetric flow sensors, or γ -ray technology-based grain photoelectric yield sensors. These sensors require continuous dynamic measurements and are affected by various factors, such as the moisture content of grains, species, yield differences, harvesting speed, and variations in flow rate due to vehicle adjustments at the ground level. These factors can lead to large measurement errors (De *et al.*, 2020; Jensen *et al.*, 2019; Sun *et al.*, 2022; Liu *et al.*, 2022). At the same time, these yield detection methods need to be calibrated before operation. Conventional calibration methods require correction by weighing on the ground for comparison. Moreover, with the change of time and space, frequent calibration is also necessary. Calibration difficulties cause detection inaccuracies. This system combines sensor strengths: load cells for large masses, photoelectric sensors for small ones. It calibrates photoelectric sensors with load cell data, improving per - unit yield measurement accuracy.

MATERIALS AND METHODS

Yield Monitoring System Principle

The principle of yield measurement using weighing method is to add a pressure transducer directly underneath the grain tank of the harvester and convert the weight of the grain applied to the transducer into an electrical signal (Hong *et al.*, 2019).

The working principle of the load cell is shown in Figure 1(b), where R_1, R_2, R_3 and R_4 are resistive strain gauges. When the load cell is subjected to gravity, it undergoes slight deformation. The strain gauges also deform under external force, leading to changes in their resistance values. These changes follow a specific relationship with the applied force. By measuring the variation in resistance, the magnitude of the external force can be accurately determined.

$$U = \frac{R_1 R_3 - R_2 R_4}{(R_1 + R_2)(R_3 + R_4)} U_0 \quad (1)$$

where U_0 is the DC supply voltage, and U is the output voltage. In the formula above, the resistance values of the four resistors are the same. When the sensor strain gauge is subjected to external forces, the resistance values change, and the output voltage will also change. Therefore, the amount of change in the voltage can be taken as an indication of the change in the resistance values, as a way to determine the force acting on the elastic element.

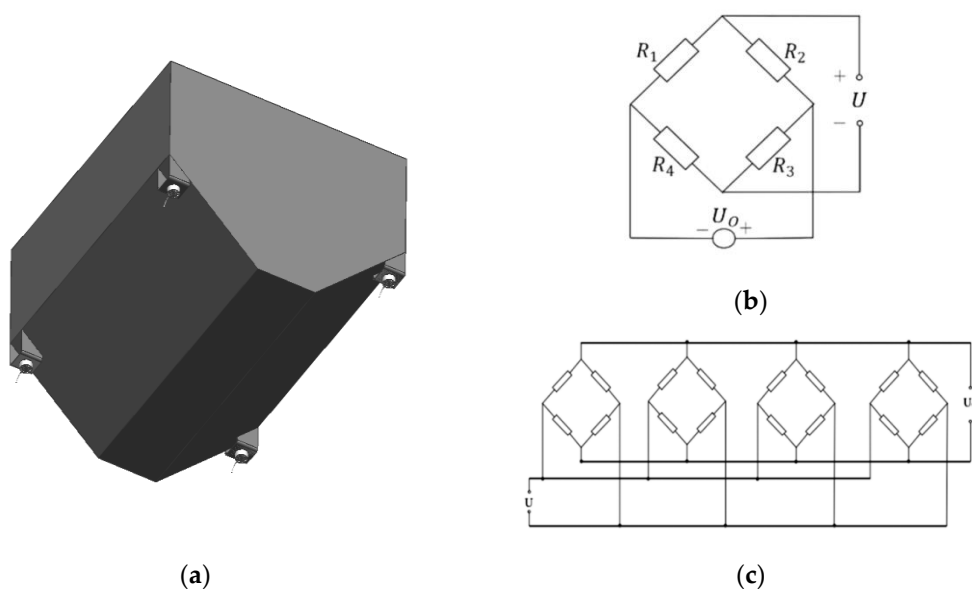


Fig. 1 - Installation position of the four load cells at the bottom of the grain tank

Designed according to the volume and shape of the harvester's grain tank, a weighing structure uses four load cells to measure the weight of the wheat in the tank. Each load cell needs to be placed on the same level during installation, otherwise the measurement quality will be inaccurate. Multiple load cells will output multiple signals, in order to streamline the wiring and the controller, a weighing structure only needs to collect one weighing signal, which can be connected to four load cells in series or in parallel (Marangoni *et al.*, 2017). Due to the poor stability of the series connection, the system uses the parallel connection for the 4 load cells, as shown in Figure 1(c). After connecting the pressure sensor with the transmitter, the RS485 to USB converter is used to connect the transmitter with the host computer, and the host computer data acquisition software receives, displays, stores and analyzes the collected data.

The light transmitter and light receiver of the opposed-radiation photoelectric sensor are on the same axis installed on both sides of the scraper lifter, respectively, and when the grain passes through the photoelectric path of the sensor, the photoelectric path is blocked, which causes the output voltage of the light receiver to change potentiometrically (Jin *et al.*, 2022). Therefore, the thickness of the grain on the scraper is determined by recording the duration of the output pulse signal of the photoelectric sensor, and the measurement of the grain mass is finalized based on the bottom area of the scraper and the grain capacity weight. The principle is shown in Figure 2(b).

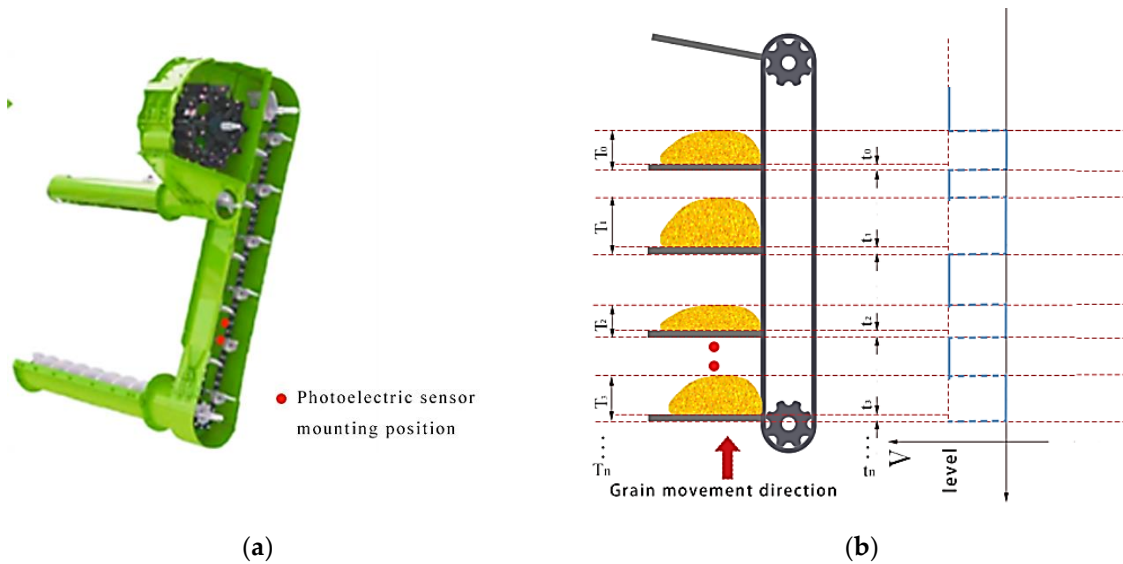


Fig. 2 - Photoelectric Sensor Yield Measurement Principle

where T_n is the time when the infrared rays of the opposed-beam photoelectric sensor are blocked by the grain and the scraper, and t_n is the time when the scraper blocks the sensor, and the sensor outputs a low-level signal. By counting the time of the low-level signal output from the opposed-beam photoelectric sensor, the yield estimation model constructed in this paper is used to obtain the weight of the grain entering the bin in the combine harvester.

When the combine harvester is operating under normal working conditions, the wheat yield M_1 is measured by the photoelectric yield monitoring system. Once it reaches the preset threshold, the load cell weighs the wheat in the grain tank to obtain M_2 , and the feedback unit calculates the calibration coefficient K .

$$K = \frac{M_2}{M_1} \tag{2}$$

where: K is the photoelectric metering calibration coefficient; M_1 is the mass measured by the photoelectric sensor; M_2 is the mass measured by the load cell. After the load cell weighs the grain in the tank, it calculates the new photoelectric metering coefficient. The system then updates the old coefficient with the newly calculated one and stores it for use in the next yield measurement.

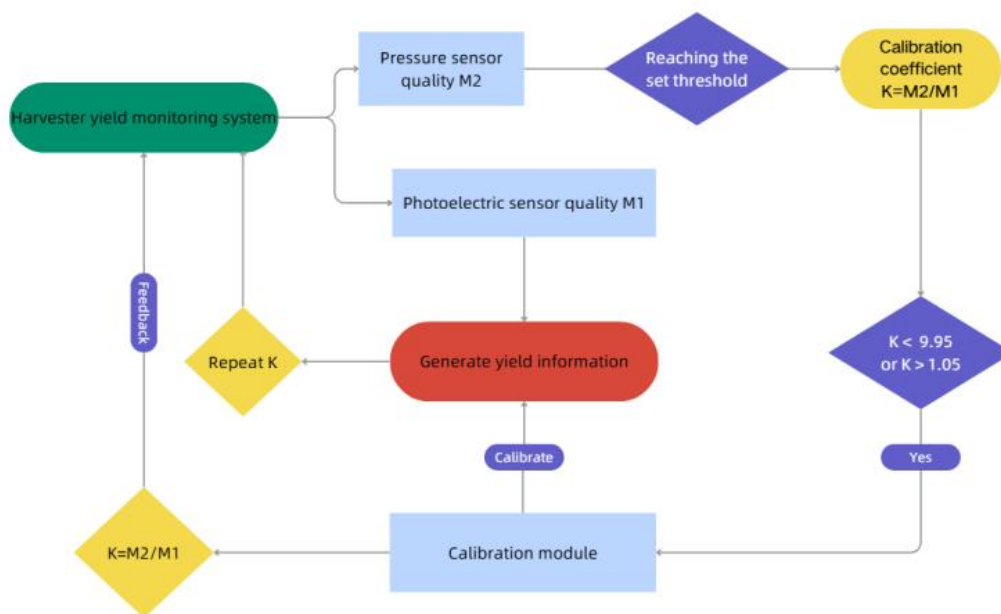


Fig. 3 - Workflow of the yield monitoring calibration system

Yield Monitoring System Hardware Selection

The yield monitoring system is installed on the grain combine harvester, which mainly collects crop yield information in real time. It mainly includes main control module, sensor module, data transmission module, digital signal processing and model conversion module, power supply module, data storage and display unit, etc., as shown in Figure 4.

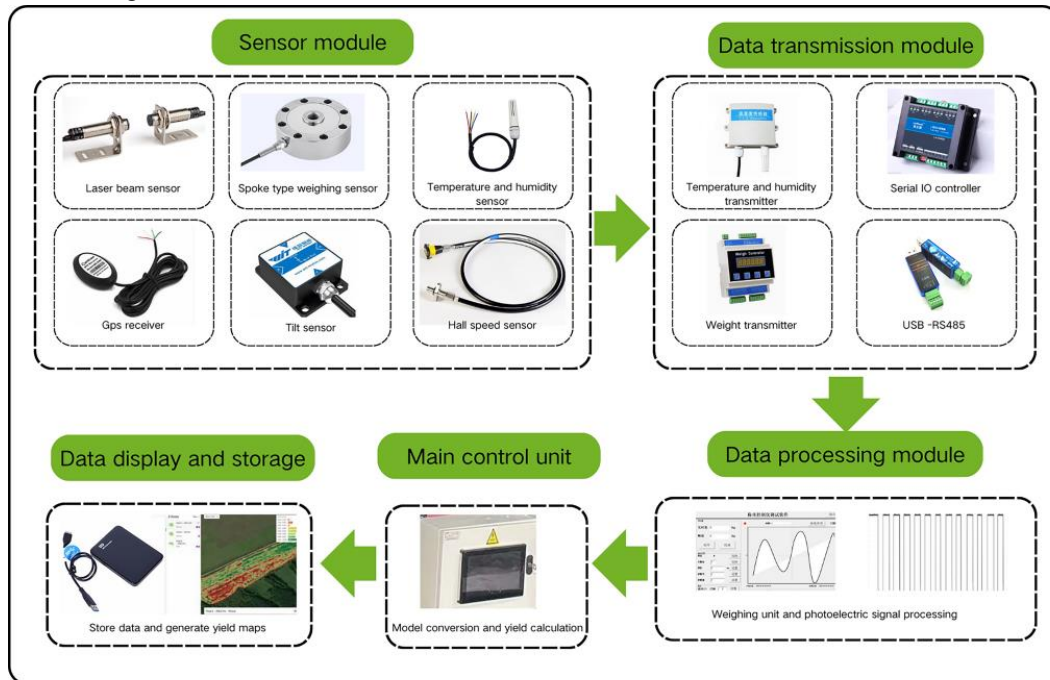


Fig. 4 - Schematic diagram of the harvester yield monitoring system

After passing through the harvester cleaning device, wheat grains are conveyed by a screw conveyor at the harvester's bottom to a scraper - type elevator. The scraper elevator, composed of a scraper, chain, and shell, uses the chain - moving scraper to lift grains to the harvester's grain tank. To study grain quality in the tank and the relationship between photoelectric sensor output and grain quality, a yield monitoring test bed was designed based on the 4YZL - 6S harvester elevator (Figure 5). The test bench includes a bottom screw conveyor, scraper elevator, top screw conveyor, grain tank, drive mechanism, and control system. The elevator is at a 72° angle to the ground. During operation, harvested wheat reaches the scraper elevator after cleaning. Photoelectric sensors at the elevator bottom estimate grain quality by recording pulse - signal durations from wheat shading, combined with scraper parameters. Pressure sensors under the grain bin convert grain weight to electrical signals, and data is sent to the host computer. When the photoelectric yield monitoring system reaches a set threshold, the pressure sensor weighs, calculates calibration coefficients, calibrates the photoelectric sensor, and generates yield information for real - time crop yield monitoring.

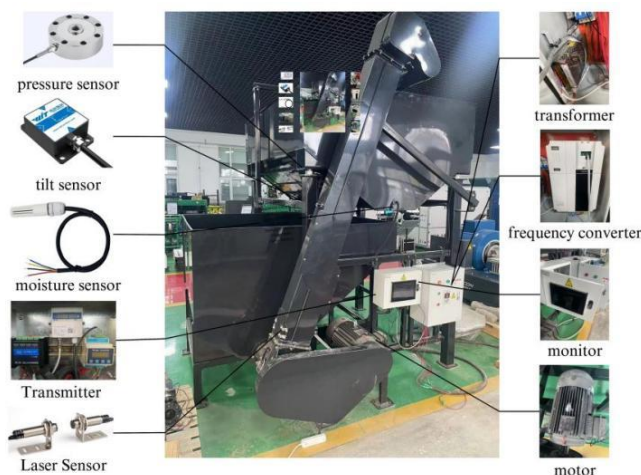


Fig. 5 - Yield monitoring system test bench structure

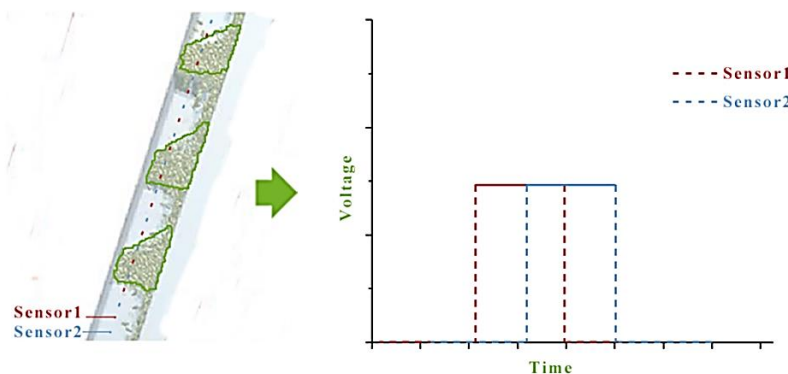
In order to obtain the relationship between the duration of photoelectric signal and the quality of grain, as well as the load pressure of the grain box on the counterweight sensor, this paper carries out the selection of hardware for the test bench. Two counter-reflective photoelectric sensors, specifically the E2F-20C2 (NPN) type, were selected and placed at the bottom of the scraper lifter. These sensors, manufactured by Wenzhou Mingxun Electronics Co., Ltd. (Wenzhou, China), have a supply voltage range of 6 – 36 V and a response time of ≤ 2 ms. The photoelectric sensors' data transmission module is selected to be the serial IO controller of LangHande, with a supply voltage of 9–24 V, and adopts the standard Modbus- RTU protocol of the relay. The load cell used is the SLLF-74 spoke-type load cell, manufactured by Shenglong Machinery Co., Ltd. (Wenzhou, China), with a measurement range of 1 T and a power supply requirement of 5–12 V. The load cell transmitter is the XSF4-channel digital transmitter from Bengbu Zhongnuo Sensors Technology Co., Ltd. (Bengbu, China), which operates with a 10–30 V power supply, has a sampling frequency of 500 Hz, supports the Modbus-RTU protocol, and offers an accuracy of 0.0003%. The transmitter is connected to the host computer via an RS-485 to USB converter. The power supply unit provides 12 V through a transformer to power both the sensors and the transmitters.

Photoelectric Sensor Yield Measurement Model

Since the photoelectric sensor cannot directly obtain the grain quality, it is necessary to construct the relationship between the photoelectric signal and the quality model. For NPN-type sensors, the transmitter emits light, and when an object enters the detection area to block the light, the amount of light received by the receiver changes, and the detection circuit produces an electrical signal change according to this change. When there is no obstruction, the sensor outputs a low level; when an object blocks the light, the sensor outputs a high level, thus realizing the detection of the object. Thus, the relationship between wheat volume and the photoelectric signal can be established by calculating the cumulative generation voltage time. In order to avoid the large error data generated by a single sensor, two photoelectric sensors were selected for the experiments in this paper. However, in the process of photoelectric sensors being blocked by wheat, the scraper of the grain bin will also block the photoelectric sensors at the same time, which will have an impact on the results of yield calculation, so the time of shielding wheat particles during the accumulation of photoelectric sensors eliminates the influence of the scraper on the total accumulation time, the calculated formula is:

$$T = \sum \left(\frac{T_{an} + T_{bn}}{2} - t_n \right) \tag{3}$$

The time at which photoelectric sensor No. 1 accumulates the generated potential is denoted as T_{an} , and the time at which photoelectric sensor No. 2 accumulates the generated potential is denoted as T_{bn} . The time at which the photoelectric sensor monitors the accumulation of each scraper is represented as t_n . Additionally, T signifies the average accumulated time during which the photoelectric sensor monitors the wheat. These time parameters are critical for analyzing the sensor's response and the accumulation process of the wheat. Looking at the analysis of the accumulation of wheat on the elevator by EDEM 2022.2 software, it can be approximated that the accumulation pattern of wheat on each scraper is close to a trapezoidal shape, as shown in Figure 6.



(a)

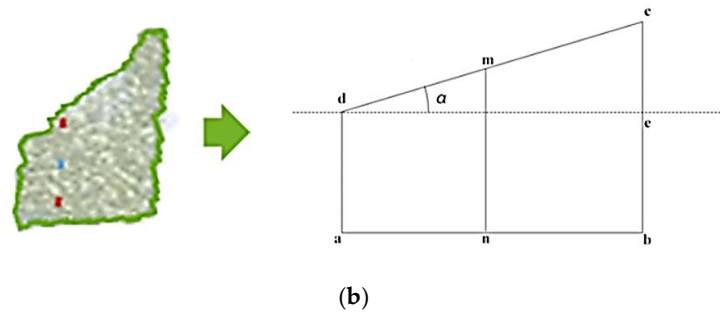


Fig. 6 - Relationship between wheat volume and potential

Since the scrapers are rigidly connected to the elevator chain, the spacing between each scraper is nearly identical. Given that the length and width of each scraper are fixed, a linear relationship exists between the volume of grain on each scraper and the stacking height of the grain. Therefore, the mass of grain on each scraper can be estimated by monitoring the duration for which the wheat obstructs the photoelectric sensors and combining this information with the elevator's speed. The volume of grain on a scraper is calculated as:

$$V = L_{ab}L_{mn} + \left(\frac{L_{nb}^2 \tan \alpha}{2} - \frac{L_{an}^2 \tan \alpha}{2} \right) L_1 \tag{4}$$

where L_{ab} is the width of the scraper, L_1 is the length of the scraper, L_{mn} is the photoelectric sensor monitoring line, which can be understood as the effective length of the grain that can be monitored by the photoelectric sensor during the scraper lifting process. L_{an} is the length from the sensor monitoring line mn to the upper edge of the scraper, L_{nb} is the length from the sensor monitoring line mn to the lower edge of the scraper, α is the angle of the top of the grain pile relative to the scraper. From Equation (5), it can be seen that there is a linear relationship between the stacked volume of grain and the measured value of photoelectric sensor L_{mn} under the ideal model. However, the yield monitoring system in this paper is calibrated to the thickness of the scraper after idling, when L_{mn} is 0 the volume V of the grain is also 0, and the value of the constant term in Equation (4) is 0. Therefore, the mass m of the grain measured in the system is positively proportional to the cumulative voltage time corresponding to L_{mn} and the mass of the wheat is given in the Equation (5):

$$m = kL_{mn} \tag{5}$$

where k is the coefficient of positive proportionality of the cumulative voltage generation time to m .

Weighing System Correction Model

To address errors from uneven terrain in field operations, a mathematical model between tilt angle and weighing error is established. Nonlinear regression fits experimental data, and a compensation algorithm for tilted grain bins is proposed. The photoelectric sensor data model is better calibrated by enhancing load cell stability. When the grain box is stationary on the ground (0°), the sensor output equals the actual wheat mass. When the grain box is tilted, the load cell is in a tilt - weighing state. As shown in Figure (7), the force on the sensor at this time is:

$$\begin{cases} F_2 = W_m \cos \alpha \\ F_3 = W_m \sin \alpha \end{cases} \tag{6}$$

where F_2 is the load of the load cell along the vertical direction of the grain tank, and F_3 is the load of the load cell along the horizontal direction of the grain tank, F_2 is the main direction force of the load cell, which is perpendicular to the pressure sensor and has a good linear relationship, while F_3 is the parallel direction force of the load cell, whose output is affected by the tilt direction of the grain tank, the mass of the wheat W_m , the angle of inclination α and other factors. From equation 7, the output of the load cell at this time is:

$$W_s = F_2 + f(F_3) = W_m \cos \alpha + f(W_m \sin \alpha) \tag{7}$$

where: W_s is the output value of the pressure transducer, $f(F_3)$ is the nonlinear function that affects the output of the pressure transducer. According to equation (6) and (7), it can be inferred that:

$$W_e = W_m - W_s = W_m(1 - \cos\alpha) - f(F_3) \tag{8}$$

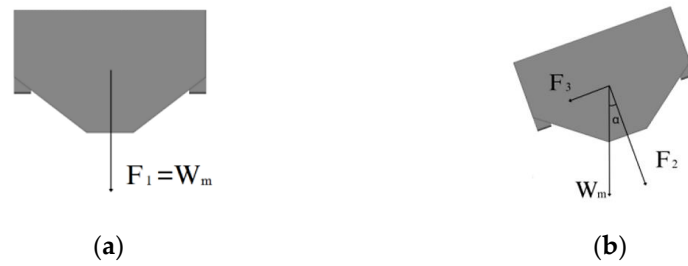


Fig. 7 - Grain box force analysis

When the grain bin is at a certain angle to the ground, Equation (8) is decomposed by the Taylor's equation:

$$W_e = W_m \left(\frac{1}{2}\alpha^2 + o(\alpha^2) \right) - f(F_3) \tag{9}$$

In this equation, $o(\alpha^2)$ represents the second order infinitesimal quantity of α . Since the effect of $o(\alpha^2)$ in Equation (9) on the load weight value is very small, it can be neglected. Based on this, the weighing error compensation equation can be derived:

$$W'_m = W_s + W_e = W_m \left(1 + \frac{1}{2}\alpha^2 \right) - f(F_3) \tag{10}$$

where W'_m is the weight compensated according to the algorithm. Due to the complexity of the change of the force plane of the load cell and the insensitivity of the force F_3 in the horizontal direction of the sensor to the action of the load cell, Equation (11) can be simplified as follows.

$$W'_m = K_2 \cdot W_s \cdot \alpha^2 + B \tag{11}$$

where K_2 is the tilt compensation coefficient, B is the model correction value. Due to the insensitivity of the weighing pressure sensor to lateral stress. In this paper, simplifying the model, correcting the tilt direction according to the change of tilt angle of the load cell caused by the load of the grain tank, and then compensating the weighing accuracy according to the corrected tilt angle are considered.

RESULTS

Determination of the coefficient of proportionality

To get the positive coefficient k between cumulative potential generation time and wheat quality, experiments were done on a designed bench. Shandong Luzhong's Qimin 13 hulled wheat (moisture 12 - 14%, purity 98%) was used. Instruments included Yingheng T1 scale, Shandong Huali motor, and Shandong Shenchuan inverter. Test photos are shown in Figure 9.

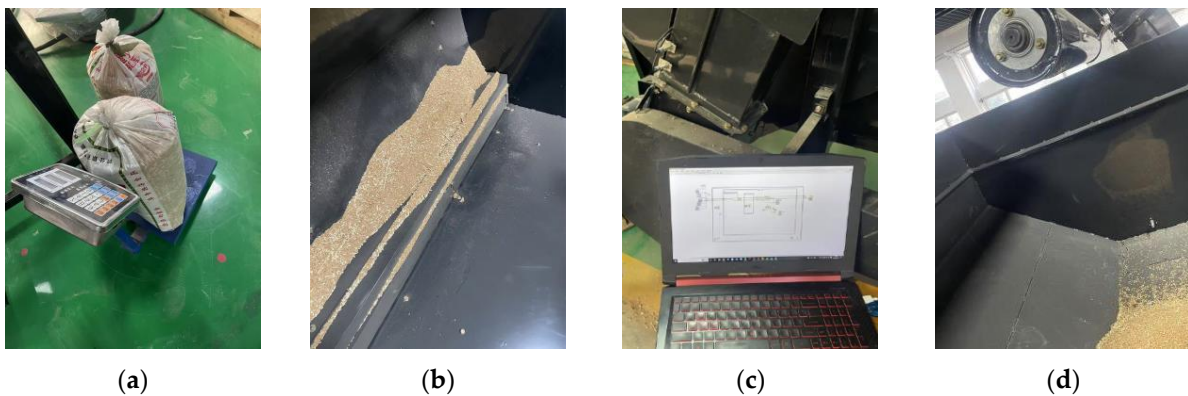


Fig. 8 - Indoor bench experiment site

To determine the proportionality coefficient under different scraper lifter speed conditions, 30 sets of tests were conducted at motor frequency converter settings of 10 Hz (approximately 150 r/min), 20 Hz (approximately 300 r/min), and 25 Hz (approximately 375 r/min). For each test, the system recorded the accumulated photoelectric signal duration along with the actual grain mass measured by a bench scale. The results are shown in Figure 9.

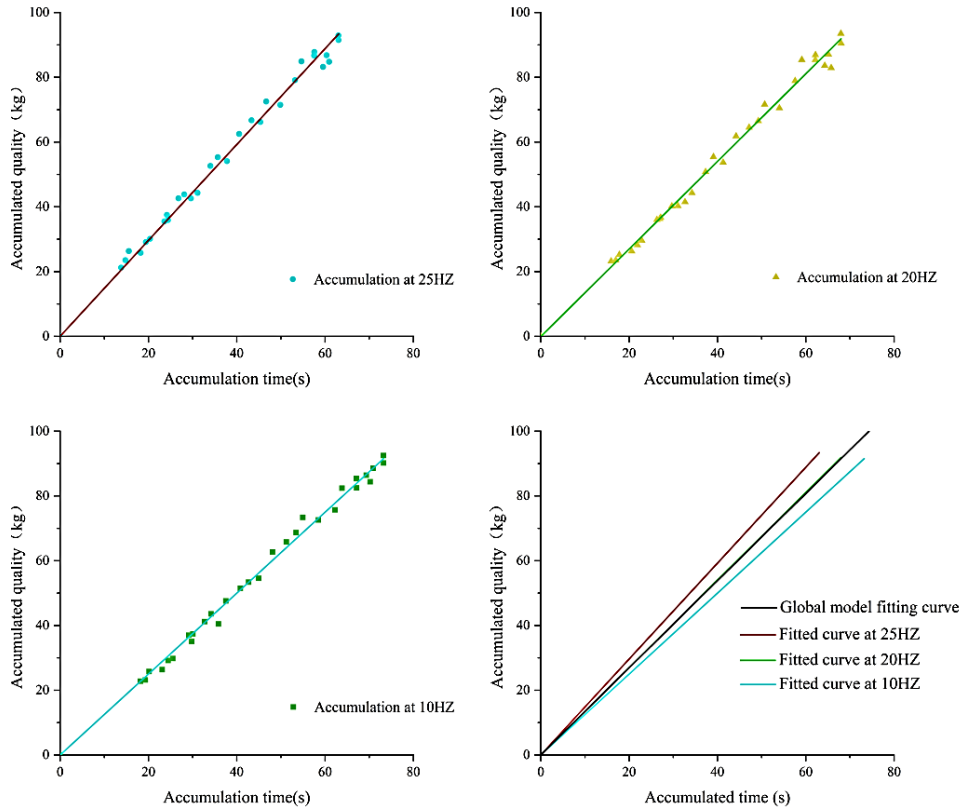


Fig. 9 - Fitted straight line between cumulative time and mass at different rotational speeds

Since the experiment has been calibrated for the cumulative time of the scraper pair in the unloaded state of the scraper lifter at each frequency, each frequency has the constraint that the constant term of the fitted curve is 0. Based on the experimental results, the cumulative time was fitted to the actual weighing mass of the grain by linear regression using Origin2024 software, and the following positive scale factors were obtained, respectively:

The positive proportionality coefficient at 25 Hz (approx.375 r/min) is:

$$M = 1.370(T_1 + T_2) \tag{12}$$

The positive proportionality coefficient at 20 Hz (approx.300 r/min) is:

$$M = 1.362(T_1 + T_2) \tag{13}$$

The positive proportionality coefficient at 10 Hz (approx.150r/min) is:

$$M = 1.349(T_1 + T_2) \tag{14}$$

Positive scale factor for global model:

$$M = 1.355(T_1 + T_2) \tag{15}$$

where $T_1 + T_2$ represents the total duration of the output signals from the two photoelectric sensors. Based on this relationship, the positive scale factor k is determined to be 1.355. The fitted model achieved correlation coefficients of 0.998, 0.992, 0.994, and 0.994.

Weighing error compensation

To study the impact of load cell weighing errors in the grain bin under different tilt angles, this research adjusted the yield test stand using a manual forklift to angles of 0.5°, 1°, and 1.5°. A total of 1000 kg of grain was loaded into the test stand, with sampling points set every 200 kg to calculate the error at each point. Before the experiment, the grain box was leveled using the HWT901B tilt angle sensor from Witte Intelligent Technology Co., Ltd. (Shenzhen, China). The motor frequency was set to 20 Hz, and 200 kg of wheat was added to the bottom grain bin. The cumulative time of the potential generated by the photoelectric sensor was recorded to determine the actual mass of wheat using a model conversion factor. After the wheat was transferred to the top grain bin, the mass measured by the load cell was collected. Due to gaps between the scraper elevator and screw conveyor, the measured mass was less than 200 kg, requiring manual replenishment until the load cell reading reached 200 kg.

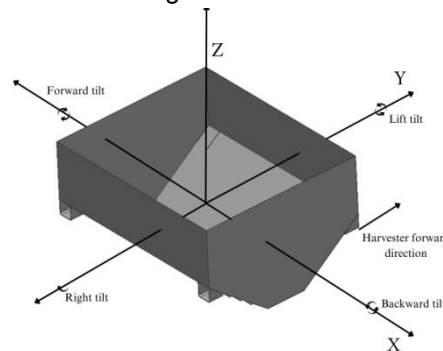


Fig. 10 - Schematic diagram of the adjustment direction of the laboratory bench

In practice, grain distribution in the bin is non-uniform. When the harvester tilts, the thickness of the grain pile and the position of the center of gravity shift in the left, right, or forward/backward directions. These variations, along with the mechanical structure of the harvester and sensor placement, influence the measurements. The harvester's structure may exhibit varying stiffness and flexibility in different directions, leading to differential deformation around the load cell when tilted. Additionally, despite precise mounting, slight variations in the sensitivity or response characteristics of the load cells in different directions may persist. These combined factors contribute to discrepancies in readings when tilted in various directions.

To address this, a forklift was used to fill the test stand from all four directions, adjusting it to the appropriate angles to collect weight and angle data from the grain bin. The weighing error under tilted conditions was determined by comparing the sensor-measured mass of wheat with the actual mass loaded. After completing the experiment at one sampling point, the process was repeated for the remaining points. The experimental results are presented in Figure 11.

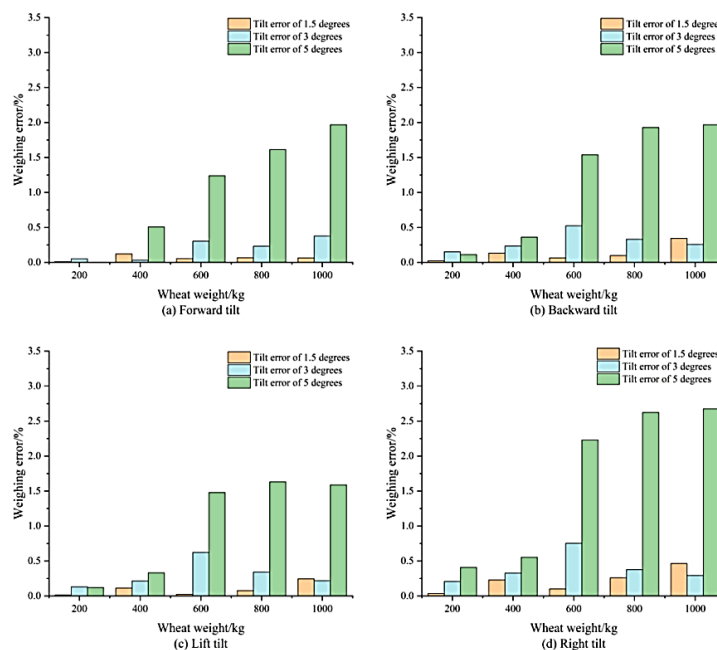


Fig. 11 - Weighing errors in different directions and at different angles of inclination

The experimental results show that the weighing error of the bin is almost negligible when the tilt angle is 0.5° . However, when the tilt angle reached 1.5° , the weighing errors in the four directions increased significantly, far exceeding the error levels of 0.5° and 1° . The analysis shows that the weighing accuracy of the bin under the left tilt condition is slightly higher than that of the other directions, which may be related to the inhomogeneity of wheat distribution in the bin. When the grain bin is tilted to the right, the grains on the left side may become more densely packed due to gravity, while the right side remains relatively loose. This causes the force on the right-side sensor to increase. Conversely, when the bin is tilted to the left, the inlet located on the right side promotes a more uniform grain distribution within the bin, thereby reducing the measurement error. For forward and backward tilts, the feeding port remains aligned with both directions, resulting in relatively similar errors in both cases. To improve weighing accuracy under inclined ground conditions, this paper proposes a corresponding error compensation algorithm for the grain bin.

To determine the tilt compensation coefficient K_2 and the model correction value in Equation (11), and to correct for the influence of inclination on the model, this study utilizes load cell weighing data collected under tilted conditions. The model parameters are fitted using the least-squares algorithm.

$$S = \sum_{i=1}^n (y_i - f(x_i))^2 \quad (16)$$

where S is the sum of squared errors, representing the total of the squared differences between the model's predicted value y_i and the true observed value $f(x_i)$. The objective of the least squares method is to minimize S in order to determine the optimal parameters of the model. Here, y_i is the observed value of the i -th sample, based on the model function f , when the input is the independent variable x_i of the i -th sample.

Considering that the measurement error is small and close to the accuracy error of the load cell itself when the tilt angle is 0.5° and 1° , this paper only compensates the weighing error for the weighing data with tilt angle of 1.5° under single-axis tilt condition. Where $K_2 = 0.44$, $B = -1.93$. The fitting accuracy is 0.818. In addition, the error plots for both corrected and uncorrected tilt angles are compared in this paper, as shown in Figure 12.

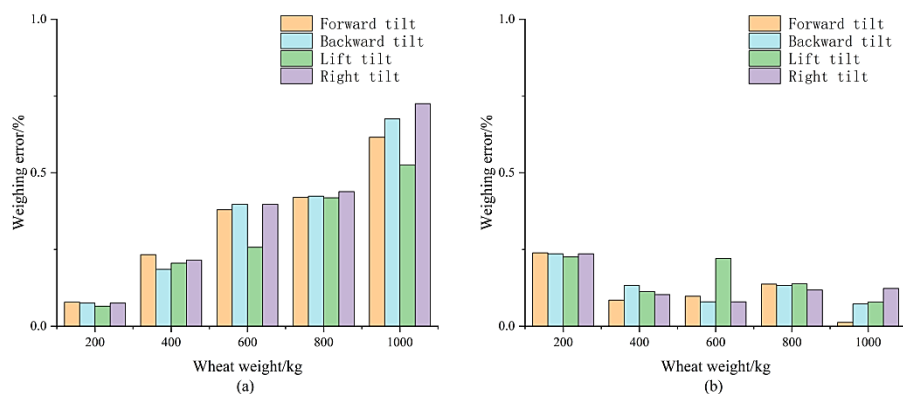


Fig. 12 - Plot of uncorrected model vs corrected model

From the comparison, it can be observed that the compensation accuracy and consistency of the model without tilt angle correction decrease as the loading load increases. In contrast, the compensation performance of the model with tilt angle correction improves progressively with increasing load. The overall error after compensation remains below 0.25%, and the accuracy of the corrected model consistently surpasses that of the uncorrected model. Overall, the compensation effect of the corrected model is significantly better than that of the uncompensated approach.

Experimental Results of a Self-Feedback Labor Monitoring System

In order to verify the accuracy of the model based on the improved photoelectric yield monitoring system, this paper simulates the harvester field operation by indoor bench test. The data of the photoelectric yield monitoring system and weighing system were obtained by manually inputting wheat into the bottom grain bin, and the test was conducted by inputting in batches of 200 kg into the grain inlet of the test stand. The calibration accuracy of the pressure sensing was set to 200 kg, and the yield quality corresponding to the global fitting coefficients was used to measure the yield. The excellence with the self-feedback system was contrasted, and the results of the experiments are shown in Table 1.

Table 1

Photogrammetric production data without the addition of a calibration system

Frequency /Hz	Quality of Inputs/kg														
	200			400			600			800			1000		
	Time /s	Mass /kg	Errors /%	Time /s	Mass /kg	Errors /%	Time /s	Mass /kg	Errors /%	Time /s	Mass /kg	Errors /%	Time /s	Mass /kg	Errors /%
10	146.92	196.88	1.56	306.66	410.92	2.73	466.71	625.39	4.23	629.34	843.32	5.42	794.29	1064.35	6.44
20	147.51	197.67	1.17	305.46	409.32	2.33	463.72	621.39	3.57	625.16	837.72	4.72	785.27	1052.26	5.23
25	146.40	196.17	1.91	306.00	410.04	2.51	464.42	622.33	3.72	625.98	838.82	4.85	788.25	1056.26	5.63

Table 2

Photometric data added to the calibration system

Frequency /Hz	Quality of Inputs/kg														
	200			400			600			800			1000		
	Time /s	Mass /kg	Errors /%	Time /s	Mass /kg	Errors /%	Time /s	Mass /kg	Errors /%	Time /s	Mass /kg	Errors /%	Time /s	Mass /kg	Errors /%
10	146.92	196.88	1.56	299.50	401.33	0.33	448.99	601.65	0.28	599.56	803.42	0.43	750.16	1005.21	0.52
20	147.51	197.67	1.17	299.21	400.94	0.23	449.25	602.00	0.33	598.78	802.37	0.30	749.38	1004.17	0.42
25	146.40	196.17	1.91	299.60	401.47	0.37	448.36	600.80	0.13	599.01	802.68	0.34	751.77	1007.37	0.74

The yield monitoring system with the addition of the self-feedback module is clearly shown by the experimental results to have a certain compensation effect at all three frequencies, and the before and after comparison with the error without the feedback module is shown in Figure 13.

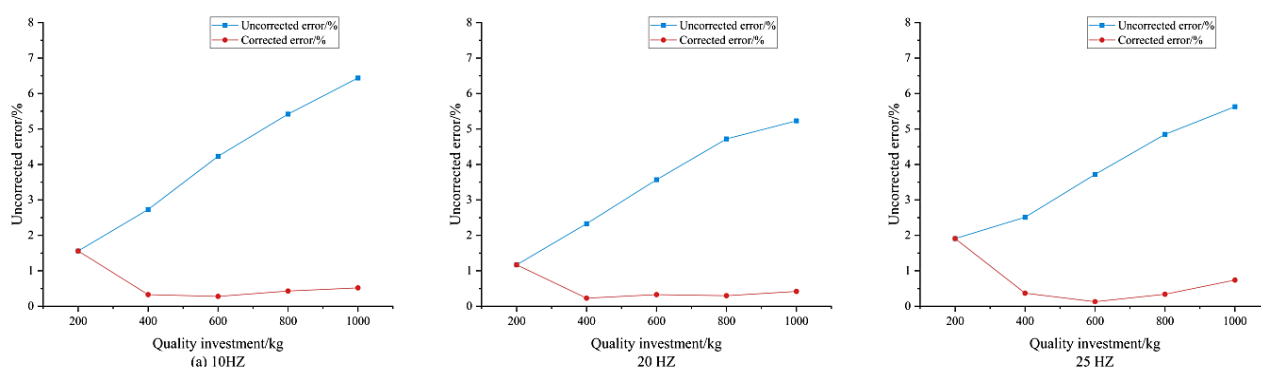


Fig. 13 - Comparison of yield data with and without calibration system

As shown by the results, the error is relatively large when the input is 200 kg. This is because the load cell's calibration accuracy is set for 200 kg, and the threshold for calibration had not yet been reached, meaning the feedback module had not been activated. At this stage, the photoelectric measurement coefficient remains at its initial value. Once the input reaches 400 kg, the system's self-feedback module begins functioning, correcting the photoelectric measurement coefficient. Observations from the 2nd to 5th tests show that the system's yield measurement error gradually stabilizes, with errors ranging from 0.23% to 0.74%. The optimal

calibration occurs at a frequency converter setting of 20 Hz, where the overall error remains below 0.42%, indicating strong accuracy and stability of the system. In contrast, the standalone photoelectric yield measurement system exhibits a larger error fluctuation range, between 1.17% and 6.44%, with a tendency for errors to increase over time. The self-feedback calibration system effectively performs dynamic calibration, keeping the error within a stable range. This significantly reduces system fluctuations and measurement errors, thereby ensuring the accuracy and stability of the system.

CONCLUSIONS

In this study, a multi-sensor fusion-based yield monitoring system for grain harvesters was successfully designed and validated, and a series of results of significant value were obtained. The positive proportionality coefficients between the photoelectric signal and the grain mass at different rotational speeds were determined through experiments, and the overall error of the system was less than 6.44% in the initial test. The established model of the relationship between tilt angle and weighing accuracy and the compensation algorithm were effective, with the overall error less than 0.25% after compensation and less than 0.74% after system intervention. The self-feedback calibration system played a key role in keeping the system error low under different loads, and the best calibration effect was achieved at 20 Hz, with the overall error less than 0.42%. The system provides an efficient and reliable yield monitoring solution for agricultural production, which strongly promotes the development of precision agriculture and helps to improve resource utilization efficiency and economic benefits. However, considering the complexity of practical applications, more field trials are needed in the future to further optimize the adaptability of the system to different environments and crops, and to improve the sensor parameters and algorithms, so as to give full play to the potential of the system in agricultural production and help agriculture achieve higher quality development.

ACKNOWLEDGEMENT

This article was supported by a grant from the Development of High Efficiency and Low Loss Single Longitudinal Axial Flow Threshing and Separation Technology and Intelligent Flexible Threshing Device Project, Grant No. 2021YFD200050204.

REFERENCES

- [1] Cheng S., Han H., Qi J., Ma, Q., (2023) Design and Experiment of Real-Time Grain Yield Monitoring System for Corn Kernel Harvester (玉米籽粒收获机实时谷物产量监测系统的设计与实验) *Agriculture*, Vol.13, 294. <https://doi.org/10.3390/agriculture13020294>
- [2] Choi, M.C., Lee, K.H., Jang, B.E., (2018) Grain Flow Rate Sensing for a 55 Kw Full-Feed Type Multi-Purpose Combine. *Int. J. Agric. Biol. Eng*, Vol. 11, pp. 206–210. <https://doi.org/10.25165/j.ijabe.20181105.2686>
- [3] De Queiroz, D.M., Coelho, A.L.D., Valente, D.S.M., Schueller, J.K. (2020) Sensors Applied to Digital Agriculture: A Review. *Rev. Cienc. Agron.* 51, e20207751.
- [4] Fang Y., Chen Z., Wu L., (2024) Design and Experiments of a Convex Curved Surface Type Grain Yield Monitoring System. (凸曲面型谷物产量监测系统的设计与实验) *Electronics*, Vol.13, 254. <https://doi.org/10.3390/electronics13020254>
- [5] Geng D., Tan D., Su G., (2021) Optimization and Experimental Verification of Grain Yield Monitoring System Based on Pressure Sensors. (压力式谷物产量监测系统的验证与优化) *Trans. Chin. Soc. Agric. Eng*, Vol.37, pp.245–252.
- [6] Hong, Y.D., Lee, B. (2019) Logarithmic Strain Model for Nonlinear Load Cell. *Sensors*, 19, 3486. <https://doi.org/10.3390/s19163486>.
- [7] Jensen, J.A., Garmendia, A.G. (2019) Comparison between Bin Tonnages and Yield Monitor Predictions. *Int. Sugar J.* Vol.121, pp. 272-277.
- [8] Jin C., Cai Z., Yang T. (2022) Design and Experiment of Yield Monitoring System of Grain Combine Harvester. (谷物联合收割机产量监测系统的设计与实验) *Trans. Chin. Soc. Agric. Mach.* Vol.53, pp.125–135.
- [9] Li M., (2004). The Technique of Crop Yield Monitor and Key Equipment Agric (作物产量监测技术及关键设备农业). *Agriculture Network Information*. pp. 34–38.

- [10] Liu R., Sun Y., Li M., (2022) Development and Application Experiments of a Grain Yield Monitoring System. (谷物产量监测系统的开发与应用实验) *Comput. Electron. Agric*, Vol.195, 106851. <https://doi.org/10.1016/j.compag.2022.106851>.
- [11] Luo X., Zang Y., Zhou Z., (2006) Research Progress in Farming Information Acquisition Technique for Precision Agriculture (精准农业中农业信息获取技术的研究进展). *Trans. Chin. Soc. Agric. Engineering*, Vol. 22, pp. 167–173. Guangdong/China.
- [12] Luo X., Zhang T., Hong T. (2001). Technical System and Application of Precision Agriculture(精准农业的技术系统及应用). *Transactions of the Chinese Society for Agricultural Machinery*, Vol.32, pp. 103-106, Guangdong/China.
- [13] Maldaner, L.F., Canata, T.F., Molin, J.P. (2022). An Approach to Sugarcane Yield Estimation Using Sensors in the Harvester and Zigbee Technology. *Sugar Tech*, Vol.24, pp. 813–821.
- [14] Maldaner, L.F., Corrêdo, L.D., Canata, T.F., (2021). Predicting the Sugarcane Yield in Real-Time by Harvester Engine Parameters and Machine Learning Approaches. *Comput. Electron. Agric.* 181, 105945. SP/Piracicaba <https://doi.org/10.1016/j.compag.2020.105945>
- [15] Marangoni, R.R., Rahneberg, I., Hilbrunner, F., Theska, R., Fröhlich, T. (2017). Analysis of Weighing Cells Based on the Principle of Electromagnetic Force Compensation. *Measurement Science and Technology*. 28, 075101. <https://doi.org/10.1088/1361-6501/aa6bcd>
- [16] Martello, M., Molin, J.P., Bazame, H.C. (2022) Obtaining and Validating High-Density Coffee Yield Data. *Horticulturae*, Vol.8, 421. <https://doi.org/10.3390/horticulturae8050421>
- [17] Momin, M.A., Grift, T.E., Valente, D.S., Hansen, A.C. (2019) Sugarcane Yield Mapping Based on Vehicle Tracking. *Precis. Agric*, Vol.20, pp.896–910. <https://doi.org/10.1007/s11119-018-9621-2>
- [18] Navid, H., Taylor, R.K., Yazgi, A., (2015) Detecting Grain Flow Rate Using a Laser Scanner. *Trans. ASABE*, Vol.58, pp.1185–1190.
- [19] Price, R.R., Johnson, R.M., Viator, R.P. (2017). An Overhead Optical Yield Monitor for a Sugarcane Harvester Based on Two Optical Distance Sensors Mounted above the Loading Elevator. *Appl. Eng. Agric*. Vol.33, pp. 687–693. <https://doi.org/10.13031/aea.12191>
- [20] Sirikun, C., Samseemoung, G., Soni, P., Langkapin, J., Srinonchat, J. (2021) A Grain Yield Sensor for Yield Mapping with Local Rice Combine Harvester. *Agriculture*, 11, 897. <https://doi.org/10.3390/agriculture11090897>
- [21] Sun Y., Liu R., Zhang M., Li M., (2022) Design of Feed Rate Monitoring System and Estimation Method for Yield Distribution Information on Combine Harvester. *Comput. Electron. Agric*, 201, 107322. <https://doi.org/10.1016/j.compag.2022.107322>
- [22] Taylor, J.A., Sanchez, L., Sams, B., (2016) Evaluation of a Commercial Grape Yield Monitor for Use Mid-Season and at-Harvest. *J. Int. Sci. Vigne Vin*, Vol. 50, pp. 57–63.
- [23] Wang H., Bai X., Liang H. (2017) Proportional Distribution Method for Estimating Actual Grain Flow under Combine Harvester Dynamics. (联合收割机动态下实际粮食流量估算的比例分配方法). *Int. J. Agric. Biol. Eng.* Vol.10, pp.158–164. <https://doi.org/10.25165/j.ijabe.20171004.2732>
- [24] Wang S., Yu Z., Zang W., (2021) Review of Recent Advances in Online Yield Monitoring for Grain Combine Harvester (谷物联合收割机在线产量监测研究进展) *Trans. Chin. Soc. Agric. Eng*, Vol. 37, pp.58-70.
- [25] Yin C., Zhang Q., Mao X., (2024) Research of Real-Time Corn Yield Monitoring System with DNN-Based Prediction Model (基于 DNN 的实时玉米产量监测系统研究). *Front. Plant Sci*, 15, 1453823. <https://doi.org/10.3389/fpls.2024.1453823>
- [26] Zandonadi, R.S., Stombaugh, T.S., Shearer, S.A., (2009) Laboratory Performance of a Mass Flow Sensor for Dry Edible Bean Harvesters. *Appl. Eng. Agric*. Vol. 26, pp.11–20.